Geophysical Research Letters®

Key Points:

- The shape of the active length (L) versus discharge (Q) relation mirrors the distribution of specific subsurface capacity along the network
- The $L(Q)$ law can be reconstructed combining observations of active length and discharge collected during different time periods
- We derive exact analytical expressions that connect the $L(Q)$ law to the distributions of local persistency, flowrate and active length

Supporting Information:

Supporting Information may be found in the online version of this article.

Correspondence to:

N. Durighetto,
nicola.durighetto@unipd.it

On the Relation Between Active Network Length and Catchment Discharge

Nicola Durighetto[1] (ID) **and Gianluca Botter[1]** (ID)

[1]Department of Civil, Environmental and Architectural Engineering, University of Padua, Padova, Italy

Abstract The ever-changing hydroclimatic conditions of the landscape induce ceaseless variations in the wet channel length (L) and the streamflow (Q) of a catchment. Here we use a perceptual model to analyze the links among (and the drivers of) four descriptors commonly used to characterize discharge and active length dynamics in streams, namely the $L(Q)$ relationship and the cumulative distributions of local persistency, flowrate and active length. The model demonstrates that the shape of the $L(Q)$ law is defined by the cumulative distribution of the specific subsurface discharge capacity along the network, a finding which provides a clue for the parametrization of $L(Q)$ relations in dynamic streams. Furthermore, we show that $L(Q)$ laws can be constructed combining the streamflow distribution with disjoint active length data. Our framework links previously unconnected formulations for characterizing stream network dynamics, and offers a novel perspective to describe the scaling between wet length and discharge in rivers.

Plain Language Summary Stream networks react to changing climatic conditions (wetting or drying) in the surrounding landscape. Consequently, the length of flowing channels and the corresponding streamflow vary through time owing to precipitation events and seasonal climatic patterns. Here we present a conceptual model that analyzes the controlling factors of four standard descriptors of streamflow and active length dynamics in streams, and identifies their mutual connections. The model provides insight on the physical processes that determine the joint changes of active length and discharge, investigating the impact of climate and landscape morphology on these standard descriptors. The approach formally describes how the relation between flowrate and active length originates from the spatial aggregation of local properties of the stream network (water supply and transport capacity). A set of mathematical relations is also derived, which can be used in practical applications to interpret and predict the relationship between wet length and catchment discharge - even in cases in which synchronous measurements of these two variables are not available.

1. Introduction

Stream networks are not steady, as they expand and retract in response to changing hydrologic conditions in the surrounding landscape. Channel network dynamics are observed in a wide range of climatic settings (Datry et al., 2014; Messager et al., 2021; Skoulikidis et al., 2017) and are crucial to key in-stream biogeochemical and ecological processes (Abbott et al., 2016; Acuña et al., 2014; Berger et al., 2017; Boodoo et al., 2017; Datry et al., 2014, 2018; Dupas et al., 2019; Giezendanner et al., 2021; Nikolaidis et al., 2013; Reyjol et al., 2014; Vander Vorste et al., 2020; von Schiller et al., 2014). The link between the actively flowing length of a stream network (L) and the discharge at the corresponding outlet (Q) has long been studied in the hydrological litera-ture (Blyth & Rodda, 1973; Day, 1978; Gregory & Walling, 1968). Empirical $L(Q)$ relations have been used to quantify the sensitivity of the active length of streams to changes in the underlying hydrological conditions in selected case studies (Durighetto et al., 2022; Godsey & Kirchner, 2014; Jensen et al., 2017; Lapides et al., 2021; Prancevic & Kirchner, 2019; Senatore et al., 2020; Shaw et al., 2017; Ward et al., 2018; Zanetti et al., 2021; Zimmer & McGlynn, 2017). However, owing to the operational burden associated to river network mapping, to date the dynamics of wet length has been measured only in relatively few catchments. Furthermore, the only existing mechanistic model designed to explain the nature of the relation between Q and L is the model proposed by Prancevic and Kirchner (2019), who related the exponent of the $L(Q)$ law to measurable topographic features of a catchment. However, in Prancevic and Kirchner (2019) the functional form of the relation between the wet length and the catchment discharge was de facto prescribed as a power law, owing to the assumptions made on the scaling of the relevant hydro-morphologic features with the contributing area. Better understanding the nature and the shape of the $L(Q)$ relation in streams could help in exploiting global datasets on the temporal dynamics of the discharge to predict the sensitivity of the wet length of stream networks to rainfall and climate drivers.
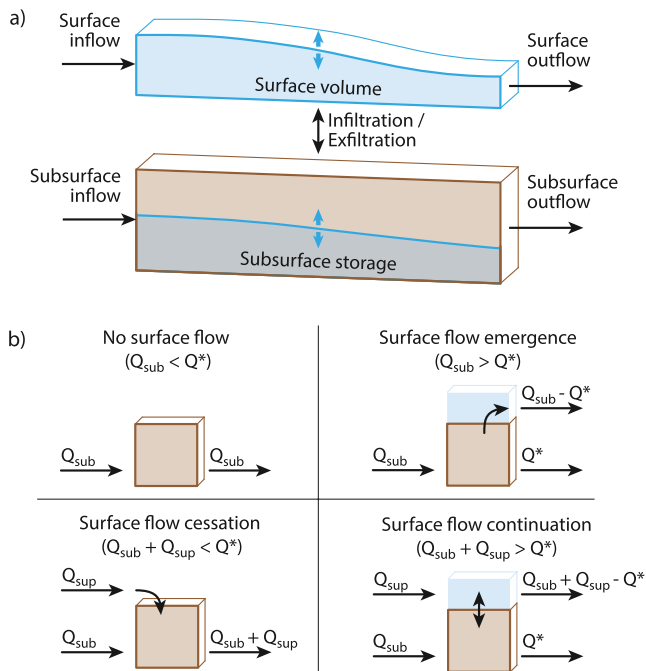
Figure 1. Scheme of the perceptual model proposed in this paper (a), and the resulting four possible cases of surface flow presence/absence. The proposed scheme is based on the concepts introduced by Godsey and Kirchner (2014).

Crucially, the $L(Q)$ relation itself does not suffice to provide an exhaustive characterization of the complex hydrological dynamics experienced by catchments where the active network responds dynamically to rainfall events and seasonal climatic patterns. Accordingly, three other descriptors have been developed in the literature to quantify the temporal dynamics of streamflow and active length in river basins, namely the flow duration curve (FDC), the stream length duration curve (SLDC) and the spatial distribution of local persistencies. The FDC, defined as the streamflow exceedance probability, has been frequently employed by hydrologists and practitioners to describe the streamflow regime, as it provides a robust quantitative basis for a variety of water resources engineering problems (Botter et al., 2008; Castellarin et al., 2004; Doulatyari et al., 2015; Foster, 1934; Vogel & Fennessey, 1994, 1995). Analogously, the SLDC, that is, the complement of the cumulative distribution function of the active length, has been recently become a standard tool to characterize the magnitude of network dynamics induced by changes in the underlying climatic conditions (Botter & Durighetto, 2020; Durighetto et al., 2022; Lapides et al., 2021). The local persistency, instead, quantifies the probability of observing surface flow in a given location within the network. Accordingly, the spatial distribution of flow persistency illustrates which portions of the stream network are more likely to experience surface runoff when the catchment wets up (e.g., Botter et al., 2021; Costigan et al., 2016). The spatial distribution of local persistency, the temporal distributions of flowrate and active length, and the L versus Q relationship provide important clues about the dominant hydrological processes operating in a landscape and can be used as a basis for classifying ephemeral and perennial streams (e.g., Costigan et al., 2017; Durighetto et al., 2022). Therefore, understanding how these descriptors are mathematically connected to each other represents an important unresolved issue in hydrology.

Here, we formalize a perceptual model for surface flow emergence suited to describe the joint dynamics of streamflow and active length in streams, seeking to address the following research questions:

1. How are the FDC, the SLDC, the spatial pattern of local persistency and the L versus Q relation connected to each other?
2. Can we disentangle climatic and morphologic signatures in these key descriptors of L and Q dynamics?
3. How does the shape of the $L(Q)$ relation reflect the spatial statistics of key physical features of the catchment?

These research questions are tackled combining theoretical analyses and a proof-of-concept application.

2. Methods

2.1. A Perceptual Model for Surface Flow Emergence

In this paper we describe the joint dynamics of stream network length and catchment-scale discharge produced by sequences of rain events or seasonal climatic patterns. The selected temporal resolution is longer than the underlying catchment concentration time - so as that changes in catchment storage produced by rain events are reflected in measurable streamflow variations at the outlet (e.g., daily to weekly timescales). In this vein, surface flow emergence can be studied via a water balance approach applied to an arbitrary stream portion of the geomorphic network (here defined as the maximum potential extension of the active network in a catchment, see Botter et al., 2021; Zimmer & McGlynn, 2017). Each stream portion has a typical size of a few meters, so as internal, fine-scale patters of surface flow can be ignored. The water balance approach accounts for the subsurface flow in the underlying permeable soil layer (or hyporheic region) and the overlying surface water flow (if any). Accordingly, the perceptual model comprises two distinct domains (i.e., the subsurface and surface volumes) that store and transport water downstream, while interacting by means of infiltration and exfiltration processes, as represented in Figure 1a.

In the search of analytical formulations, we make here the following two simplifying assumptions: (a) as the surface and subsurface domains are tightly coupled, surface flow is expected to be triggered by saturation excess developing along the geomorphic network (Dunne & Black, 1970; Tsegaw et al., 2020); (b) at the relevant temporal scales, network dynamics are seen as a sequence of steady states at different catchment wetness levels, during each of which the dynamics of the local subsurface storage are neglected. Under the above assumptions, the emergence of surface flow is linked to the imbalance between the flowrate supplied from upstream (intended as the combination of surface discharge, Q_{sup}, and subsurface flow, Q_{sub}) and the maximum subsurface transport capacity, Q^*, as proposed by Godsey and Kirchner (2014) and Prancevic and Kirchner (2019). In particular, the conceptual model incorporates four possible cases (represented clockwise in Figure 1b from the top-left corner):

1. No surface flow is observed whenever the water input is supplied only as subsurface flow ($Q_{sup} = 0$), and this flow can be transported downstream within the subsurface domain because $Q_{sub} \leq Q^*$;
2. Surface flow emergence occurs where $Q_{sub} > Q^*$, and the flowrate exceeding the subsurface transport capacity is exfiltrated;
3. Surface flow continuation is the condition in which surface flow is supplied from upstream ($Q_{sup} > 0$). In this case, surface flow increases downstream if $Q_{sub} > Q^*$ and additional water is exfiltrated from the subsurface. If $Q_{sub} < Q^*$, instead, streamflow may decrease downstream as surface water partially infiltrates. Nevertheless, as $Q_{sub} + Q_{sup} > Q^*$, surface flow is still continuing because part of the incoming water cannot be accommodated in the underlying soil;
4. Surface flow cessation is the result of the complete infiltration of the surface water produced upstream, that is observed wherever $Q_{sub} + Q_{sup} \leq Q^*$. In this case, we assume that the infiltration of surface water in the hyporheic region is not constrained by the infiltration capacity of the streambed, as Q_{sup} is relatively small ($Q_{sup} = Q^*$ in the worst scenario).

Thus, surface flow along the network is observed in the following two instances (cases 2 and 3 above): when the subsurface gets fully saturated by the incoming groundwater input; or when a fraction of the surface flow produced upstream is delivered downstream as by-pass overland flow. In the general case, the condition that determines surface flow emergence can be thus expressed as $Q_{sub} + Q_{sup} > Q^*$, as proposed by Godsey and Kirchner (2014), Prancevic and Kirchner (2019), and Lapides et al. (2021). Despite its simplicity, the local perceptual model retains the core of the coupling of surface and subsurface runoff used in spatially-explicit physically-based models (e.g., Bencala et al., 2011; Camporese et al., 2010; Ward et al., 2018).

Specifying the spatio-temporal variability of Q_{sub}, Q_{sup} and Q^* along the stream network will allow the perceptual model to be applied at the network scale. In general, monitoring the spatial and temporal patterns of Q_{sub}, Q_{sup} and Q^* is practically unfeasible. To overcome this limitation, the assumption according to which network dynamics are seen as a sequence of steady-states can be further leveraged, as described in what follows.

2.2. A Simple Analytical Model for Quantifying and Connecting the Dynamics of L and Q in Streams

In the proposed perceptual model, the presence/absence of surface flow at a given location is represented by the local status of the focus stream portion:

$$X(x,t) = \begin{cases} 1 & \text{if } Q(x,t) > Q^*(x) \\ 0 & \text{otherwise} \end{cases}, \tag{1}$$

where $X = 1$ implies the presence of flowing water and $X = 0$ corresponds to a dry section (Botter & Durighetto, 2020). In the above equation, the subsurface transport capacity $Q^*(x)$ usually refers to fully-saturated conditions and is a durable feature of each location of the study catchment determined by stationary hydro-morphological properties (e.g., saturated hydraulic conductivity, topographic gradient, transmissivity) (Lapides et al., 2021; Prancevic & Kirchner, 2019). The water flow supplied from upstream $Q(x,t)$, instead, varies both in space and time. By introducing the local specific discharge (i.e., per unit catchment area), defined as:

$$q(x,t) = Q(x,t)/A(x), \tag{2}$$

where $A(x)$ represents the upslope contributing area in the location x, Equation 1 can be rewritten as follows:

$$X(x,t) = \begin{cases} 1 & \text{if } q(x,t) > \rho^*(x) \\ 0 & \text{otherwise} \end{cases} \tag{3}$$

where $\rho^*(x) = Q^*(x)/A(x)$ is the local subsurface discharge capacity scaled to its contributing area. ρ^* represents a spatially variable threshold for the local specific inflow $q(x,t)$, above which surface flow is observed. In spite of the general nature of the above formulation (Equations 1 and 3), specifying the spatial and temporal patterns of $q(x,t)$ within the whole stream network is infeasible. To overcome this limit, and in line with what proposed by Godsey and Kirchner (2014) and Prancevic and Kirchner (2019), we assume that q is spatially uniform: $q(x,t) = q(t)$. This complies with our previous assumption, according to which network dynamics are seen as a sequence of steady-states during which subsurface storage variations are negligible. Under the assumption of uniform streamflow generation, the local flowrate is proportional to the contributing area (i.e., $Q(x,t) = A(x)q(t)$, see (2)) and $q(t)$ can be estimated as:

$$q(t) = Q(t)/A_T \tag{4}$$

where $Q(t)$ is the surface discharge at the outlet (where subsurface flows can be neglected) and A_T is the total catchment area. $Q(t)$ and $q(t)$ vary with time, mainly driven by catchment-scale hydroclimatic fluctuations. Here, the temporal variability of the hydrologic signal that forces the catchment is quantified via the cumulative distribution function of the specific discharge, CDF_q, which is computed using a derived distribution approach as:

$$CDF_q(q) = CDF_Q(q \cdot A_T) \tag{5}$$

where CDF_Q is the cumulative (non-exceedance) distribution function of the catchment streamflow. CDF_q directly relates to the FDC and denotes the probability of observing a specific discharge lower than q in the focus catchment.

The presence/absence of surface flow in a given location x, characterized by the transport capacity $\rho^*(x)$, is determined by the temporal variability of $q(t)$, as per Equation 3. In particular, the probability to observe surface flow in the location x is known as local persistency (Botter & Durighetto, 2020), and in our formulation corresponds to the probability of $q(t)$ being bigger than the threshold $\rho^*(x)$:

$$P(x) = Prob[X(x,t) = 1] = Prob\left[q(t) > \rho^*(x)\right] = 1 - CDF_q(\rho^*(x)). \tag{6}$$

The local persistency can be empirically estimated as the relative number of times in which surface flow is observed (Durighetto et al., 2020). By inverting Equation 6, $\rho^*(x)$ in a given location of the network could be estimated exploiting field observations of catchment streamflow and local probability of flow occurrence.

In the proposed framework, the total length of the active network at a given time can be obtained by integrating the status of each point along the stream network, $X(x,t)$ as:

$$L(t) = \int_0^{L_g} X(x,t)dx = \int_0^{L_g} H\left[q(t) - \rho^*(x)\right] dx, \tag{7}$$

where L_g is the geomorphic network length and $H[\cdot]$ is the Heaviside step function. This integral represents the sum of all the lengths associated to the active sites of the network, where $X(x,t) = 1$ (green bars in Figure 2). The right-hand side of the equation embeds the condition necessary for flow emergence, as dictated by Equation 3. This formulation highlights how the spatial variability of $\rho^*(x)$ determines the pattern of flow emergence and the length of the active network (Figure 2a), while the temporal variability of $q(t)$ triggers the expansion and contraction cycles of the network. Consequently, as the active network expands (retracts) stream portions activate (dry out) following a fixed sequence determined by the spatial patterns of $\rho^*(x)$, originating stream network dynamics that are strictly hierarchical, *sensu* Botter and Durighetto (2020) - as observed in many real world settings (Botter et al., 2021).

Provided that the local status of each network portion varies in time as a function of $q(t) \propto Q(t)$, a one-to-one relation between $Q(t)$ and the corresponding $L(t)$ is observed. In fact, for a given $Q(t)$ the specific discharge can
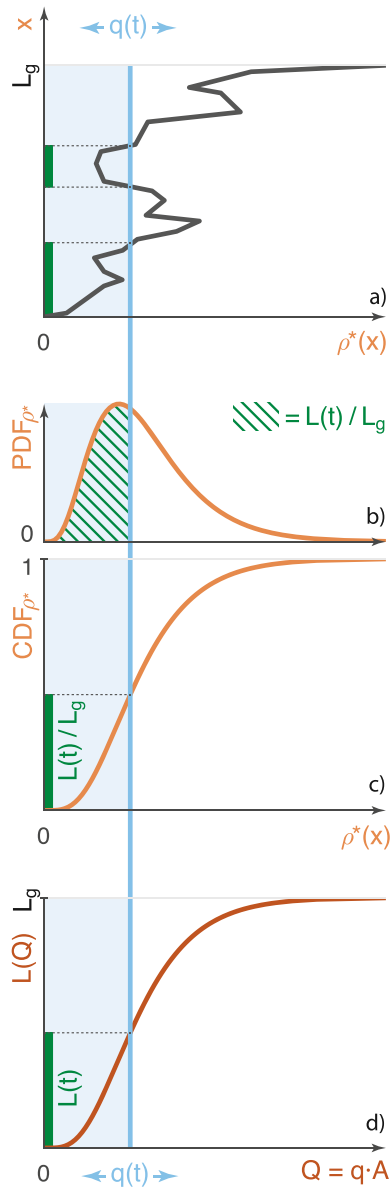
Figure 2. Spatial pattern of ρ^* (a) along a linear stream without tributaries. In this representative example, the curvilinear coordinate x traces the stream channel from the outlet ($x = 0$) to the source ($x = L_g$). The scheme could be easily generalized to branching streams. Probability density function (b) and cumulative density function (c) of ρ^*. Panel (d) shows the corresponding L-Q relation i.e., obtained by reinterpreting panel (c). Light blue shading indicates plot areas with specific discharge $<q(t)$. The green lines and hatch, instead, represent the active network (i.e., where $\rho^*(x) < q(t)$).

be calculated via Equation 4, while the active length is related to the fraction of network in which $\rho^*(x) < q(t)$ (see SI):

$$L(Q) = L_g \, CDF_{\rho^*} \left(\frac{Q}{A_T} \right) \tag{8}$$

In the above formulation, CDF_{ρ^*} is the (non-exceedance) cumulative distribution function of $\rho^*(x)$ and represents the fraction of the network in which the condition for flow emergence of Equation 3 is fulfilled (Figure 2c). Therefore, if $q(t)$ is spatially uniform, the shape of $L(Q)$ is prescribed by the cumulative distribution function (CDF) of the specific discharge capacity ρ^* (Figures 2a and 2c). In cases where $q(x, t)$ is not uniform, but the spatial patterns of the specific inflow are constant (i.e., $q(x, t) = \alpha_x(x)q_t(t)$), the result given by Equation 8 can be generalized by scaling the capacity ρ^* with the factor α_x. If the dependence of q on x and t is more complex, instead, a one-to-one $L(Q)$ law may not be identifiable. In such cases, it could be necessary to subdivide the study area into smaller and more uniform sub-catchments and describe them separately (Shaman et al., 2004; Shaw et al., 2017). Alternatively, the sensitivity of network dynamics to changes in catchment discharge can be quantified by applying a derived distribution approach (Durighetto et al., 2022) which establishes a probabilistic link between the variations of Q and L produced by time-variable hydroclimatic conditions in the contributing catchment. In particular, the active length versus discharge relation given by Equation 8 can be rewritten combining the *CDFs* of Q and L as follows (see SI):

$$L(Q) = CDF_L^{-1}\left(CDF_Q(Q)\right), \tag{9}$$

where CDF_L^{-1} is the inverse function of the cumulative distribution function of the active length, and corresponds to the SLDC (see Botter & Durighetto, 2020). In Equation 9, $CDF_Q(Q)$ quantifies the non-exceedance probability of Q, while CDF_L^{-1} relates such probability to the corresponding L. Equation 9 shows how the shape of the functional relation between L and Q can be reconstructed not only from joint observations of L and Q, but also from non-synchronous measurements of the temporal changes of streamflow and active length (as indicated in panels b, c, e of Figure 3). Furthermore, thanks to the hierarchical activation scheme implied by Equations 3 and 4, it can be proved that CDF_L directly reflects the cumulative distribution of the local persistency along the network, CDF_P (Botter & Durighetto, 2020):

$$CDF_L(L) = 1 - CDF_P^{-1}\left(1 - \frac{L}{L_g}\right), \tag{10}$$

as shown in Figure 3b. The above equation indicates that when a given fraction f of the geomorphic network is active, only all the nodes with a persistency higher than f are wet. The statistical features of surface flow presence along the network, which are quantified by $CDF_P(P)$, can in turn be expressed as a function of the CDFs of the specific discharge q and the maximum subsurface transport capacity ρ^* along the network as (see SI):

$$CDF_P(P) = CDF_{\rho^*}\left(CDF_q^{-1}(1 - P)\right), \tag{11}$$

where CDF_q^{-1} is the inverse function of CDF_q, that is, the specific FDC. In Equation 11, the term $CDF_q^{-1}(1 - P)$ is the value of q characterized by an exceedance probability equal to P (i.e., the specific flowrate exceeded for a fraction of time $= P$), while $CDF_{\rho^*}(q)$ is the fraction of nodes that are active when a discharge ($q A$) is observed at the outlet. Equation 11 shows how CDF_P, and consequently CDF_L, are the byproduct of both geomorphological properties of the catchment through CDF_{ρ^*}, and climatic characteristics of the site through CDF_q (as depicted
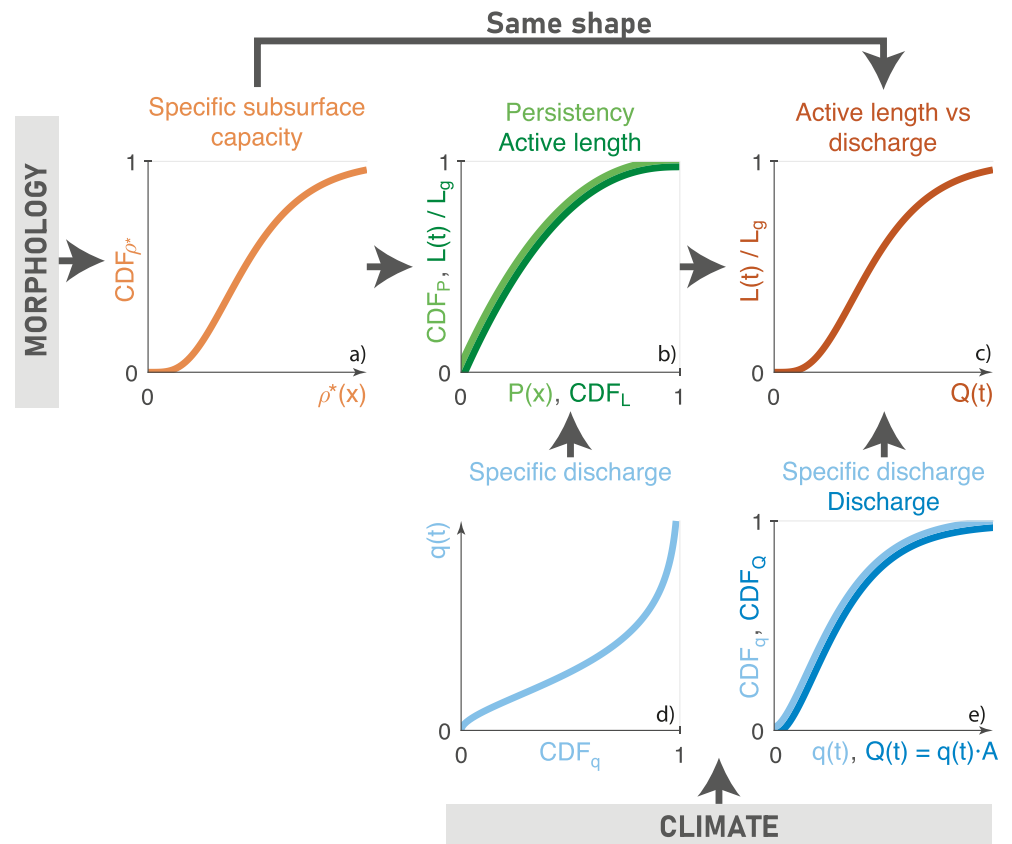
Figure 3. Graphical representation of the mathematical connections among the cumulative distribution functions of specific subsurface capacity (a), local persistency and active length (b), specific discharge (d), surface discharge (e) and the length versus discharge relation (c).

in panels a, b, d of Figure 3). Let us stress that, while Equations 8 and 11 rely on the assumptions described in Section 2.1 and the spatial uniformity of $q(t)$, Equation 9 is an analytical law with general validity. As such, it is free from any assumption and applies to all the catchments where a relation between L and Q can be identified.

3. Application to the Valfredda Catchment

To demonstrate the potential of the analytical tools developed in this paper, the proposed framework was applied to three study sites located in different regions of the world and characterized by diverse hydroclimatic properties (SI), namely the Valfredda, Poverty and Turbolo creeks. Here in the main text we report only the results for the Valfredda site, which is particularly suited to the application of the proposed approach because of the availability of active length data also during time periods in which the discharge was not monitored. The Rio Valfredda is a headwater stream in the Italian Alps draining a 5.3 km^2 high-relief catchment. The site is characterized by significant spatial heterogeneity in lithology and soil cover. A forested cover dominates the lower part of the catchment, but is quickly succeeded by grassland with large rocks, debris deposits and limestone. The geomorphic stream network is almost 17 km long, with channel widths ranging from 10 cm to 1.5 m. The stream bed mainly consists of large rocks, gravel and silt. The climate of the area is typically alpine, characterized by short, rainy summers and long, frigid winters with significant snow accumulation.

Daily discharges were measured at the outlet (diamond in Figure 4c) from November 2018 to February 2022 - with the exception of August 2020 and August–September 2021 (instrument malfunctioning). The active network was monitored through 30 visual field surveys from July 2018 to October 2021. Of these surveys, 14 were performed when discharge measurements were not available (July–October 2018, August 2020 and August–September 2021), while a total of 16 synchronous observations of active length and discharge were gathered. For more info about the catchment and the empirical activities carried out therein, the reader is referred to Durighetto
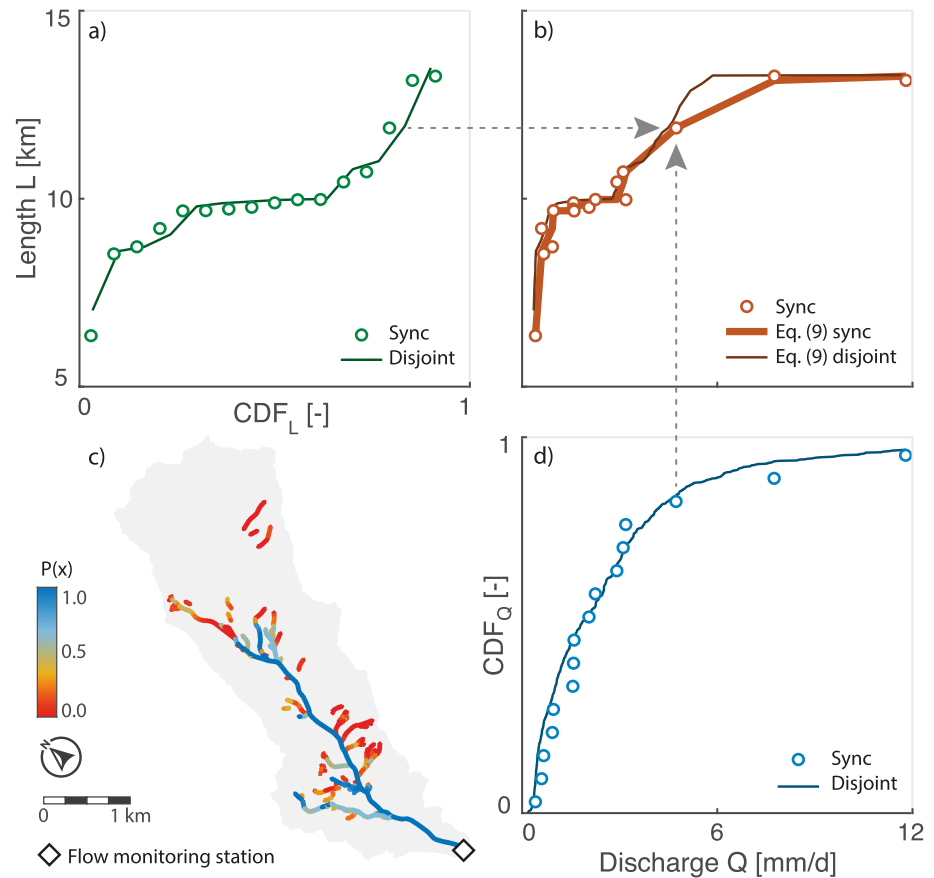
Figure 4. Map of the local persistency of the stream network in the Valfredda catchment (c). Cumulative distribution function of the active length (a), length-discharge relation (b) and cumulative distribution function of streamflow (d) of the Valfredda catchment. All CDFs were obtained with the Weibull plotting position method. The points and the thick red line refer only to joint L-Q observations, while dark thin lines refer to the remaining, disjointed, data.

et al. (2020) and Botter et al. (2021). A local persistency map was constructed on the basis of the field surveys (Figure 4c), and the Weibull plotting position method was used to construct the empirical cumulative distributions of L and Q (Figures 4a and 4d). $L(Q)$ was then obtained using three distinct methods: directly plotting synchronous empirical data in the L-Q plane, and through Equation 9 using either the 16 synchronous observations or the available non-synchronous measurements of L and Q. The empirical $L(Q)$ relationship emerging from synchronous measurements of active length and discharge can be obtained combining the x and y coordinates of the empirical points in the CDF_Q and CDF_L plots, respectively (gray arrows in Figure 4) - as prescribed by Equation 9.

The active length in the Valfredda catchment ranged from 6.3 to 13.5 km. The corresponding CDF_L is S-shaped (Figure 4a), suggesting the presence of a preferential configuration of the active network with a length of about 10 km. Nonetheless, network dynamics were quite pronounced, as the majority of the geomorphic network was dynamic. In the same period, the specific discharge ranged from 0.2 to 29 mm/d (Figure 4d). The resulting $L(Q)$ relation, shown in Figure 4b, is almost linear, except for very low (high) flows where this curve is vertical (horizontal). Equation 9 correctly traces the empirical shape of the active length - discharge relation, even when disjoint L and Q data are used to construct this curve from the CDF_Q and CDF_L. This approach, therefore, allows one to exploit datasets in which L and Q data are not perfectly synchronized (e.g., due to the practical impossibility of mapping the stream network during specific seasons or years when the discharge is instead measured, or unreliable streamflow estimations during the days in which surveys for the estimation of L are performed).

4. Discussion

In this paper, a perceptual model - wrapped around previous formulations already available in the literature, see Godsey and Kirchner (2014) - was formalized and employed to analyze the link among four descriptors commonly used to characterize the dynamics of streamflow and active length in river basins, namely the cumulative distributions of local persistency, flowrate and active length, and the L versus Q relationship. The proposed framework allowed us to provide a general, synoptic summary of all the inter-dependencies among these important catchment-scale descriptors of stream network and discharge dynamics and led to a general analytical expression for $L(Q)$, which was related to physical internal attributes of the catchment. Our analysis is effectively summarized in Figure 3, which shows how the cumulative distribution of the local persistency, the FDC, the SLDC and the $L(Q)$ law provide different yet strongly interconnected representations of the effect of climate and morphological agents on surface flow occurrence and streamflow dynamics.

Surface flow is determined by the interplay of local processes, governing the partitioning of water input in a given location between surface and subsurface flows, and spatially-integrated processes taking place in the upstream contributing catchment, that control the supply of water to the different portions of the network. By conceptualizing stream network dynamics as a sequence of stationary states at different catchment wetness levels - an assumption which is mathematically encapsulated by the spatial uniformity of $q(t)$ - the proposed model focuses on the spatial patterns of the subsurface transport capacity along the network, $\rho^*(x)$, thereby disregarding the complexity of streamflow production processes within the hillslopes. As a consequence, surface flow emergence along the network is determined by the interaction between the dynamics of the specific discharge and network-scale geomorphologic properties that control $\rho^*(x)$ (Figures 3a, 3b and 3d). According to Equation 8, the shape of $L(Q)$ can be thus interpreted as the CDF of the specific maximum discharge capacity along the network (Figures 3a and 3c). This key analytical result explains how and why morphologic and geolithologic catchment features lie at the basis of the link between L and Q (as foreseen by Prancevic and Kirchner (2019)), while climate does not produce any direct signature on the shape of active length - discharge relationship, though being directly involved in the dynamics of both L and Q (as suggested by Lapides et al. (2021), and shown in Figures 3b, 3d and 3e).

The mechanistic link between $L(Q)$ and CDF_{ρ^*} derived in this study (Equation 8) can't be straightforwardly applied to predict the shape of $L(Q)$ laws in real-world situations where active length data are not available, as $Q^*(x)$ or $\rho^*(x)$ can hardly be measured in the field. However, it offers important clues to properly parametrize the dependence of active length on catchment discharge, indicating that standard analytical distributions of positive random variables (e.g., exponential, gamma, lognormal, etc) could be efficiently used to fit empirical data of active length and catchment discharge in river basins. In this context, expressing the $L(Q)$ relation in terms of the FDC and the SLDC via Equation 9 might provide a useful alternative to characterize the functional link between Q and L in temporary streams. This alternative, however, incorporates the impact of climate, here expressed by $q(t)$, on the total active length and catchment discharge, through CDF_L and CDF_Q (Botter et al., 2021). However, when the SLDC and the FDC are combined together to define the relation between active length and catchment discharge via Equation 9, the climatic signature of these curves cancels out and the geomorphic footprint of the $L(Q)$ law emerges. The main advantage of the alternative formulation proposed in Equation 9 to characterize the nature of the $L(Q)$ relationship is the ability to exploit non-synchronous measurements of active length (or flow persistence) and catchment discharge - as shown in the example application of Figure 4b. The application of Equations 9–11 relies on a proper statistical characterization of L and Q. While we recognize the complexity of the task in case of unsteady climatic conditions, we propose that approximately 10 independent surveys carried out during the same season(s) in which the discharge is measured represent a minimum requirement to reasonably reconstruct the shape of CDF_L in a way that is consistent with the corresponding empirical CDF_Q (Botter & Durighetto, 2020).

The standard analytical model used to interpret the relationship between active length and catchment discharge is the power law model, first introduced by Gregory and Walling (1968) and then widely adopted in the literature of temporary streams (Blyth & Rodda, 1973; Day, 1978; Durighetto et al., 2022; Godsey & Kirchner, 2014; Jensen et al., 2017; Lapides et al., 2021; Prancevic & Kirchner, 2019; Senatore et al., 2020; Shaw et al., 2017; Ward et al., 2018; Zanetti et al., 2021; Zimmer & McGlynn, 2017). The power law model, however, tends to infinity when $Q \rightarrow \infty$ with a speed which is impacted also by the lower values of L and Q, and thus it might not capture cases in which the $L(Q)$ law has an horizontal plateau, for example, because the channel heads can't move upstream beyond a given point due to morphological constraints (see Figure 4, SI and Jensen et al. (2019)).

Equation 8, instead, allows a large variety of $L(Q)$ shapes - other than those enabled by a pure power-law model - an instance which makes the proposed formulation more flexible for real world applications (see Figure 4b). From this perspective, the power-law $L(Q)$ model - and its physical interpretation proposed by Prancevic and Kirchner (2019) - can be seen as a special case of Equation 7 in which all the basic quantities that define $\rho*$ are a power law function of the contributing area and the ensuing CDF of specific discharge capacity is not upwardly bounded. While appealing, the latter formulation does not account for the internal heterogeneity of morphologic and subsurface properties, which makes the active stream network disconnected in most cases - owing to the non monotonic dependence of $\rho*$ and P on the contributing area (see Figure 4b and Figures 1 and S2 in Botter et al., 2021).

5. Conclusions

In this paper, we provided general analytical relationships among four important descriptors of active length and discharge dynamics in temporary streams: the L versus Q relationship, and the cumulative distributions of local persistency, flowrate and active length. Our analysis shows mathematically how and why - while CDF_Q, CDF_L and CDF_P exhibit a climatic signature - $L(Q)$ only depends on geomorphological catchment properties. In particular, we have demonstrated that the shape of $L(Q)$ can be thought of as the CDF of the specific subsurface discharge capacity along the network. This exact result provides a clue for the efficient parametrization of $L(Q)$ relations when synchronous data of discharge and active length are available. An alternative parametrization of the $L(Q)$ law was also derived, in which local persistency or active flowing length data can be coupled to non-synchronous discharge measurements. The perceptual model formalized in this paper also clarifies that both active length and discharge dynamics are driven by other hydroclimatic covariates, here encapsulated by the temporal variability of the $q(t)$ signal. More research is needed to better characterize the physical drivers of q and $\rho*$ in stream networks, which is the goal of ongoing work.

Data Availability Statement

All the empirical data used in this study is publicly available at Durighetto and Botter (2022).

References

Abbott, B. W., Baranov, V., Mendoza-Lera, C., Nikolakopoulou, M., Harjung, A., Kolbe, T., et al. (2016). Using multi-tracer inference to move beyond single-catchment ecohydrology. *Earth-Science Reviews*, *160*, 19–42. https://doi.org/10.1016/j.earscirev.2016.06.014

Acuña, V., Datry, T., Marshall, J., Barceló, D., Dahm, C. N., Ginebreda, A., et al. (2014). Why should we care about temporary waterways? *Science*, *343*(6175), 1080–1081. https://doi.org/10.1126/science.1246666

Bencala, K. E., Gooseff, M. N., & Kimball, B. A. (2011). Rethinking hyporheic flow and transient storage to advance understanding of stream-catchment connections. *Water Resources Research*, *47*(3), 1–9. https://doi.org/10.1029/2010WR010066

Berger, E., Haase, P., Kuemmerlen, M., Leps, M., Schäfer, R. B., & Sundermann, A. (2017). Water quality variables and pollution sources shaping stream macroinvertebrate communities. *Science of the Total Environment*, *587–588*, 1–10. https://doi.org/10.1016/j.scitotenv.2017.02.031

Blyth, K., & Rodda, J. C. (1973). A stream length study. *Water Resources Research*, *9*(5), 1454–1461. https://doi.org/10.1029/WR009i005p01454

Boodoo, K. S., Trauth, N., Schmidt, C., Schelker, J., & Battin, T. J. (2017). Gravel bars are sites of increased CO_2 outgassing in stream corridors. *Scientific Reports*, *7*(1), 1–9. https://doi.org/10.1038/s41598-017-14439-0

Botter, G., & Durighetto, N. (2020). The stream length duration curve: A tool for characterizing the time variability of the flowing stream length. *Water Resources Research*, *56*(8), e2020WR027282. https://doi.org/10.1029/2020WR027282

Botter, G., Vingiani, F., Senatore, A., Jensen, C., Weiler, M., Mcguire, K., et al. (2021). Hierarchical climate-driven dynamics of the active channel length in temporary streams. *Scientific Reports*, *11*(1), 1–12. https://doi.org/10.1038/s41598-021-00922-2

Botter, G., Zanardo, S., Porporato, A., Rodriguez-Iturbe, I., & Rinaldo, A. (2008). Ecohydrological model of flow duration curves and annual minima. *Water Resources Research*, *44*(8), 1–12. https://doi.org/10.1029/2008WR006814

Camporese, M., Paniconi, C., Putti, M., & Orlandini, S. (2010). Surface-subsurface flow modeling with path-based runoff routing, boundary condition-based coupling, and assimilation of multisource observation data. *Water Resources Research*, *46*(2), W02512. https://doi.org/10.1029/2008WR007536

Castellarin, A., Vogel, R. M., & Brath, A. (2004). A stochastic index flow model of flow duration curves. *Water Resources Research*, *40*(3), 1–10. https://doi.org/10.1029/2003WR002524

Costigan, K. H., Jaeger, K. L., Goss, C. W., Fritz, K. M., & Goebel, P. C. (2016). Understanding controls on flow permanence in intermittent rivers to aid ecological research: Integrating meteorology, geology and land cover. *Ecohydrology*, *9*(7), 1141–1153. https://doi.org/10.1002/eco.1712

Costigan, K. H., Kennard, M. J., Leigh, C., Sauquet, E., Datry, T., & Boulton, A. J. (2017). *Chapter 2.2 - Flow regimes in intermittent rivers and ephemeral streams*. Academic Press.

Datry, T., Foulquier, A., Corti, R., Von Schiller, D., Tockner, K., Mendoza-Lera, C., et al. (2018). A global analysis of terrestrial plant litter dynamics in non-perennial waterways. *Nature Geoscience*, *11*(7), 497–503. https://doi.org/10.1038/s41561-018-0134-4

Datry, T., Larned, S. T., & Tockner, K. (2014). Intermittent rivers: A challenge for freshwater ecology. *BioScience*, *64*(3), 229–235. https://doi.org/10.1093/biosci/bit027

Day, D. G. (1978). Drainage density changes during rainfall. *Earth Surface Processes and Landforms*, *3*(3), 319–326. https://doi.org/10.1002/esp.3290030310

Doulatyari, B., Betterle, A., Basso, S., Biswal, B., Schirmer, M., & Botter, G. (2015). Predicting streamflow distributions and flow duration curves from landscape and climate. *Advances in Water Resources*, *83*, 285–298. https://doi.org/10.1016/j.advwatres.2015.06.013

Dunne, T., & Black, R. D. (1970). An experimental investigation of runoff production. *Water Resources Research*, *6*(2), 478–490. https://doi.org/10.1029/WR006i002p00478

Dupas, R., Abbott, B. W., Minaudo, C., & Fovet, O. (2019). Distribution of landscape units within catchments influences nutrient export dynamics. *Frontiers in Environmental Science*, *7*(APR), 1–8. https://doi.org/10.3389/fenvs.2019.00043

Durighetto, N., & Botter, G. (2022). On the relationship between active network length and catchment discharge - Dataset [Dataset]. Research Data Unipd. Retrieved from http://researchdata.cab.unipd.it/id/eprint/636

Durighetto, N., Mariotto, V., Zanetti, F., Mcguire, K. J., Mendicino, G., Senatore, A., & Botter, G. (2022). Probabilistic description of streamflow and active length regimes in rivers water resources research. *Water Resources Research*, *58*(4), 1–24. https://doi.org/10.1029/2021WR031344

Durighetto, N., Vingiani, F., Bertassello, L. E., Camporese, M., & Botter, G. (2020). Intraseasonal drainage network dynamics in a headwater catchment of the Italian Alps. *Water Resources Research*, *56*(4), e2019WR025563. https://doi.org/10.1029/2019WR025563

Foster, H. A. (1934). *Duration curves* (Vol. 99). Transactions of the American Society of Civil Engineers. https://doi.org/10.1061/TACEAT.0004522

Giezendanner, J., Benettin, P., Durighetto, N., Botter, G., & Rinaldo, A. (2021). A note on the role of seasonal expansions and contractions of the flowing fluvial network on metapopulation persistence. *Water Resources Research*, *57*(11), 1–18. https://doi.org/10.1029/2021wr029813

Godsey, S. E., & Kirchner, J. W. (2014). Dynamic, discontinuous stream networks: Hydrologically driven variations in active drainage density, flowing channels and stream order. *Hydrological Processes*, *28*(23), 5791–5803. https://doi.org/10.1002/hyp.10310

Gregory, K. J., & Walling, D. E. (1968). The variation of drainage density within a catchment. *International Association of Scientific Hydrology Bulletin*, *13*(2), 61–68. https://doi.org/10.1080/02626666809493583

Jensen, C. K., McGuire, K. J., McLaughlin, D. L., & Scott, D. T. (2019). Quantifying spatiotemporal variation in headwater stream length using flow intermittency sensors. *Environmental Monitoring and Assessment*, *191*(4), 191–226. https://doi.org/10.1007/s10661-019-7373-8

Jensen, C. K., McGuire, K. J., & Prince, P. S. (2017). Headwater stream length dynamics across four physiographic provinces of the Appalachian Highlands. *Hydrological Processes*, *31*(19), 3350–3363. https://doi.org/10.1002/hyp.11259

Lapides, D. A., Leclerc, C. D., Moidu, H., Dralle, D. N., & Hahm, W. J. (2021). Variability of headwater stream network extents controlled by flow regime and network hydraulic scaling. *Hydrological Processes*, *35*(3), e14079. https://doi.org/10.1002/hyp.14079

Messager, M. L., Lehner, B., Cockburn, C., Lamouroux, N., Pella, H., Snelder, T., et al. (2021). Global prevalence of non-perennial rivers and streams. *Nature*, *594*(7863), 391–397. https://doi.org/10.1038/s41586-021-03565-5

Nikolaidis, N. P., Demetropoulou, L., Froebrich, J., Jacobs, C., Gallart, F., Prat, N., et al. (2013). Towards sustainable management of Mediterranean river basins: Policy recommendations on management aspects of temporary streams. *Water Policy*, *15*(5), 830–849. https://doi.org/10.2166/wp.2013.158

Prancevic, J. P., & Kirchner, J. W. (2019). Topographic controls on the extension and retraction of flowing streams. *Geophysical Research Letters*, *46*(4), 2084–2092. https://doi.org/10.1029/2018GL081799

Reyjol, Y., Argillier, C., Bonne, W., Borja, A., Buijse, A. D., Cardoso, A. C., et al. (2014). Assessing the ecological status in the context of the European Water Framework Directive: Where do we go now? *Science of the Total Environment*, *497–498*, 332–344. https://doi.org/10.1016/j.scitotenv.2014.07.119

Senatore, A., Micieli, M., Liotti, A., Durighetto, N., Botter, G., Mendicino, G., & Botter, G. (2020). Monitoring and modeling drainage network contraction and dry down in Mediterranean headwater catchments. *Water Resources Research*, *57*(6), e2020WR028741. https://doi.org/10.1029/2020WR028741

Shaman, J., Stieglitz, M., & Burns, D. (2004). Are big basins just the sum of small catchments? *Hydrological Processes*, *18*(16), 3195–3206. https://doi.org/10.1002/hyp.5739

Shaw, S. B., Bonville, D. B., & Chandler, D. G. (2017). Combining observations of channel network contraction and spatial discharge variation to inform spatial controls on baseflow in Birch Creek, Catskill Mountains, USA. *Journal of Hydrology: Regional Studies*, *12*, 1–12. https://doi.org/10.1016/j.ejrh.2017.03.003

Skoulikidis, N. T., Sabater, S., Datry, T., Morais, M. M., Buffagni, A., Dörflinger, G., et al. (2017). Non-perennial Mediterranean rivers in Europe: Status, pressures, and challenges for research and management. *Science of the Total Environment*, *577*, 1–18. https://doi.org/10.1016/j.scitotenv.2016.10.147

Tsegaw, A. T., Skaugen, T., Alfredsen, K., & Muthanna, T. M. (2020). A dynamic river network method for the prediction of floods using a parsimonious rainfall-runoff model. *Hydrology Research*, *51*(2), 146–168. https://doi.org/10.2166/nh.2019.003

Vander Vorste, R., Sarremejane, R., Datry, T., Vorste, R. V., Sarremejane, R., & Datry, T. (2020). *Intermittent rivers and ephemeral streams: A unique biome with important contributions to biodiversity and ecosystem services* (Vol. 4). Elsevier Inc. https://doi.org/10.1016/b978-0-12-409548-9.12054-8

Vogel, R. M., & Fennessey, N. M. (1994). Flow duration curves I: New interpretation and confidence intervals. *Journal of Water Resources Planning and Management*, *120*(4), 485–504. https://doi.org/10.1061/(asce)0733-9496(1994)120:4(485)

Vogel, R. M., & Fennessey, N. M. (1995). Flow Duration Curves II: A Review of Applications in Water Resources Planning. *JAWRA Journal of the American Water Resources Association*, *31*(6), 1029–1039. https://doi.org/10.1111/j.1752-1688.1995.tb03419.x

von Schiller, D., Marcé, R., Obrador, B., Gómez-Gener, L., Casas-Ruiz, J. P., Acuña, V., & Koschorreck, M. (2014). Carbon dioxide emissions from dry watercourses. *Inland Waters*, *4*(4), 377–382. https://doi.org/10.5268/IW-4.4.746

Ward, A. S., Schmadel, N. M., & Wondzell, S. M. (2018). Simulation of dynamic expansion, contraction, and connectivity in a mountain stream network. *Advances in Water Resources*, *114*, 64–82. https://doi.org/10.1016/j.advwatres.2018.01.018

Zanetti, F., Durighetto, N., Vingiani, F., & Botter, G. (2021). Analysing river network dynamics and active length - Discharge relationship using water presence sensors. *Hydrology and Earth System Sciences*, *26*, 3497–3516. https://doi.org/10.5194/hess-2021-103

Zimmer, M. A., & McGlynn, B. L. (2017). Ephemeral and intermittent runoff generation processes in a low relief, highly weathered catchment. *Water Resources Research*, *53*(8), 7055–7077. https://doi.org/10.1002/2016WR019742